Comparing the spatio-temporal variability of remotely sensed oceanographic parameters between the Arabian Sea and Bay of Bengal throughout a decade

Sourav Das[1],*, Abhra Chanda[1], Suparna Dey[1], Sanjibani Banerjee[1], Anirban Mukhopadhyay[1], Anirban Akhand[1], Amit Ghosh[1], Subhajit Ghosh[1], Sugata Hazra[1], D. Mitra[2], Aneesh A. Lotliker[3], K. H. Rao[4], S. B. Choudhury[4] and V. K. Dadhwal[4]

[1]School of Oceanographic Studies, Jadavpur University, 188 Raja S. C. Mullick Road, Kolkata 700 032, India
[2]Indian Institute of Remote Sensing, 4, Kalidas Road, Dehradun 248 001, India
[3]Indian National Centre for Ocean Information Services, Kukatpally, Hyderabad 500 090, India
[4]National Remote Sensing Centre, Balanagar, Hyderabad 500 042, India

The spatio-temporal variability of sea-surface temperature (SST), photosynthetically active radiation (PAR), chlorophyll-*a* (Chl-*a*), particulate organic carbon (POC) and particulate inorganic carbon (PIC) was evaluated in the Arabian Sea (ABS) and Bay of Bengal (BoB), from July 2002 to November 2014 by means of remotely sensed monthly composite Aqua MODIS level-3 data having a spatial resolution of 4.63 km. Throughout the time period under consideration, the surface waters of ABS ($27.76 \pm 1.12°C$) were slightly cooler than BoB ($28.93 \pm 0.76°C$); this was observed during all the seasons. On the contrary, the availability of PAR was higher in ABS (45.76 ± 3.41 mol m^{-2} d^{-1}) compared to BoB (41.75 ± 3.75 mol m^{-2} d^{-1}), and its spatial dynamics in the two basins was mainly regulated by cloud cover and turbidity of the water column. The magnitude and variability of Chl-*a* concentration were substantially higher in ABS (0.487 ± 0.984 mg m^{-3}), compared to BoB (0.187 ± 0.243 mg m^{-3}), and spatially higher values were observed near the coastal waters. Both POC and PIC exhibited higher magnitudes in ABS compared to BoB; however, the difference was substantially high in case of POC. None of the parameters showed any significant temporal trend during the 12-year span, except PIC, which exhibited a significant decreasing trend in ABS.

Keywords: Marine ecosystems, oceanographic parameters, remote sensing, river basins, spatio-temporal variability.

ENVIRONMENTAL attributes like chlorophyll-*a* (Chl-*a*), sea-surface temperature (SST), particulate organic carbon (POC), particulate inorganic carbon (PIC) and photosynthetically active radiation (PAR) are the key parameters for monitoring the bio-geochemical status of marine ecosystems[1], their large-scale spatio-temporal information can only be obtained by means of satellite remote sensing[2]. The photosynthetic pigment, Chl-*a*, is a key indicator of phytoplankton biomass, which happens to be an essential biochemical characteristic of marine ecosystems, and hence, its assessment is extremely crucial for monitoring water quality of such ecosystems[3]. Likewise, SST has tremendous significance from the perspective of convection over the oceans, and especially in countries like India, where it solely governs the monsoonal rainfall and hence the entire climate variability[4]. POC and PIC in the marine environment, act as principal sources for heterotrophic organisms to degrade upon[5] and as they get degraded, nutrients are released which in turn pivot essential lifeforms of the ocean[6]. This makes the understanding of particulate carbon dynamics a crucial aspect of oceanography.

The northern end of the Indian Ocean mainly encompasses the Bay of Bengal (BoB), adjoining the east coast of the Indian subcontinent, and the Arabian Sea (ABS) on the west. Despite the fact that these two basins experience a similar geographical setting, the hydrographic and biogeochemical attributes often vary substantially[7]. The two basins are distinctively different in terms of the freshwater influx. ABS, which mainly receives the discharge from major rivers like the Indus, Narmada and Tapti, accounts for a low river run-off total of 0.3×10^{12} m^{-3} year^{-1}, while BoB receives an enormous quantity of freshwater from the rivers like Ganges, Brahmaputra, Meghna, Godavari, Mahanadi, Krishna and Cauvery, and amounts to a total run-off of 1.6×10^{12} m^{-3} year^{-1} (refs 7–9). Due to this contrasting feature, the surface waters of BoB are 3–7 psu less saline than those of ABS. Gill[11] observed an average rainfall of >2 m per year in BoB, leading to precipitation

*For correspondence. (e-mail: sourav.biooptics@gmail.com)

in excess of evaporation and hence lowering of the surface salinity to the range ~22–33 psu (ref. 12). On the contrary, in ABS evaporation dominates over precipitation causing higher salinity (~36 psu) in surface waters[13]. Moreover, in terms of suspended sediment discharge, BoB (1.4×10^9 tonnes $year^{-1}$) outruns ABS (2.0×10^8 tonnes $year^{-1}$) by a huge margin[14].

The moderate resolution imaging spectroradiometer (MODIS), has provided an opportunity to monitor 70% of the Earth's surface which is covered by the ocean. Additionally, it substantially contributes to the decadal-scale time-series data, necessary for global change and climate change assessments in the ocean[15,16]. MODIS, a major NASA Earth observation system (OAS) instrument, was launched on-board the Terra satellite on 18 December 1999, whose equator crossing time is 1030 h (descending). A similar instrument was launched for the EOS-Aqua satellite on 4 May 2002 with 1330 h equator crossing time, ascending. These two satellites have been launched for global monitoring of atmosphere, terrestrial ecosystem and the ocean, complementing each other by providing observations in the late morning and early afternoon[17]. MODIS level-1 and level-2 are 5-min 'swath' granules, while level-3 includes global 'grid' maps. Only ocean level-3 binned and level-4 (primary productivity data) are in the native HDF4 format[17]. In the present study we have used the Aqua–MODIS datasets.

The objectives of the present study are threefold. First, we wanted to compare the magnitudes of the five above-mentioned parameters (SST, Chl-*a*, POC, PIC and PAR) between the eastern BoB and western ABS flank of the northern Indian Ocean. Our second objective was to reveal the spatial and seasonal variability of these parameters in the two basins throughout the 12-year study period. Third, we wanted to monitor significant temporal trend of these parameters over the last decade, if any.

Detailed methodology

Study area

ABS encompasses the northwestern sector of the Indian Ocean and covers a total area of ~3,862,000 sq. km. It is enclosed in the north by Iran and Pakistan, to the west by the Horn of Africa and the Arabian Peninsula, to the east by the Indian Peninsula and to the south it merges with the rest of the Indian Ocean. ABS has a maximum width of ~2400 km and its maximum depth is observed to be 4652 m with a mean depth of 2734 m (ref. 18). It has a connection with the Red Sea in the southwest via the Gulf of Aden through the strait of Bab-el-Mandeb, while in the northwest, the Gulf of Oman connects it with the Persian Gulf. India, Pakistan, Iran, Oman, Yemen, Somalia, Djibouti and Maldives have coastlines on ABS.

BoB on the other hand, forms the northeastern part of the Indian Ocean; it is the largest Bay in the world comprising an area of ~2,173,000 sq. km. It is bounded by India and Sri Lanka in the west, Bangladesh in the north, Myanmar and northern Malay Peninsula in the east, and like ABS it also ends in the Indian Ocean in the south. It has a maximum width of ~1610 km and an average depth of 2600 m. The maximum depth recorded is 4694 m (ref. 19). Unlike ABS which has somewhat uniform continental shelf and slope width, BoB has a wide continental shelf in the north that narrows gradually in the south. The continental slope also has a varying gradient in the north, northeast and northwestern regions, and they are cut by canyons from the major rivers draining into them like the Ganges–Brahmaputra, Krishna and Godavari canyons. Another important physiographic aspect of the Bay is the fan of sediments of the Ganges river, which is the widest (8–11 km) and thickest in the world. Figure 1 shows a map of the study area.

Data used

Monthly composite standard level-3 data of spatial resolution 4.63 km using MODIS on-board the EOS-Aqua satellite of all the five parameters, namely SST 11 μ daytime, Chl-*a* concentration, PAR, POC and PIC were downloaded from the website http://oceancolor.gsfc.nasa.gov/cgi/l3 from July 2002 to November 2014. A total of 149 months composite data were downloaded and analysed in the present study.

Image analysis strategy

As the main objective of the study, was to carry out a comparative assessment of the selected oceanographic parameters between the ABS and BoB, two separate areas of interest (aoi).shp files were prepared for both the study areas using the ArcGIS software. However, while preparing the respective aoi, a 100 km stretch from the entire coastline adjoining the two seas was deliberately omitted and not considered for the present study. There are two fundamental reasons behind such exclusion. First, it is an unambiguously established fact that the coastal waters or continental shelf waters are the most bio-geochemically active zones of the ocean, and their characteristic features substantially differ from the rest of the open sea waters[20]. Since our main intention was to extract, analyse and compare the dataset characteristic to both BoB and ABS, it would be erroneous to include the shelf waters, as it would alter the mean values of the parameters studied by a considerable margin and would not correctly represent the vast span of the two seas. Moreover, the continental shelf waters are mostly dominated by case-2 waters, i.e. where phytoplankton abundance does not solely dominate the optical properties of turbid productive waters[21]. In these waters, due to overlapping and uncorrelated absorption by dissolved organic matter and non-algal particles,
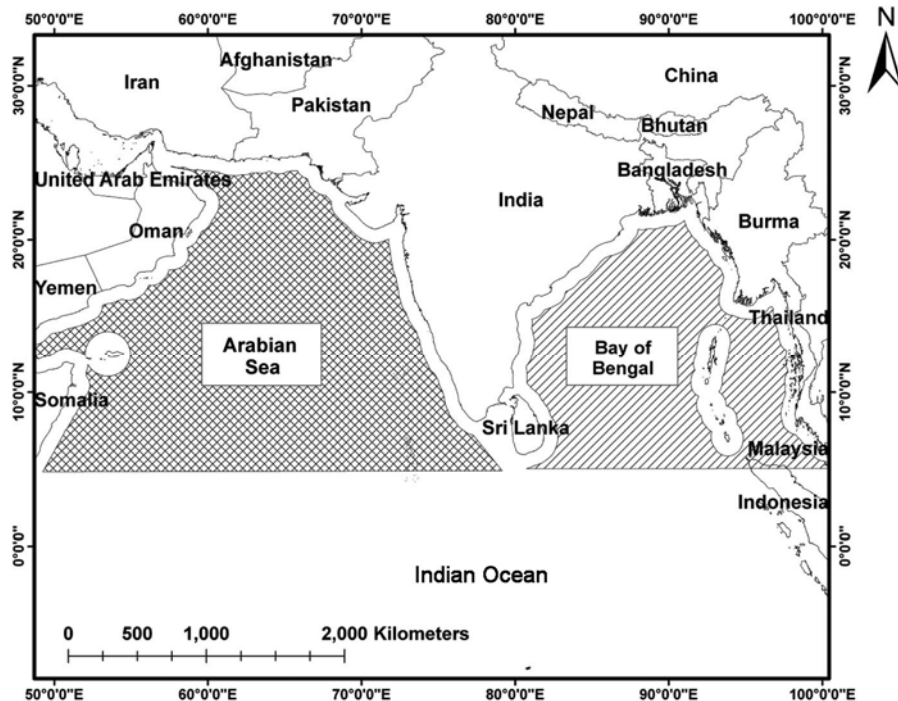
Figure 1. Map showing the area of interest (aoi) selected in the present study for the Arabian Sea (ABS) and Bay of Bengal (BoB).

chlorophyll estimation often becomes inaccurate[22,23]. However, in the open ocean waters where the observed spectral features can be directly related to chlorophyll concentrations, i.e. in case-1 waters, spectral algorithms of MODIS have been shown to yield much better estimates[24]. Owing to these reasons, the continental shelf waters were excluded from this study. The aoi considered for ABS in the present study is ~3,471,000 sq. km, while for BoB it is 2,231,000 sq. km. It is worth mentioning that in this study, we have taken into account the Andaman Sea lying adjacent to BoB.

Error rectification

All the downloaded images of the respective months were subset into two images for BoB and ABS by masking the rest of the world using the model maker of ArcGIS software (Figure 1). All the images had a fixed error value for the invalid pixels mostly due to cloud cover, and they were converted to null value so that only the cloud-free valid pixels could be taken into account while computing the statistics. The minimum, maximum, average and standard deviation of the respective month's images for all the five parameters in BoB and ABS were tabulated in Excel sheets.

Computation of seasonal composite mean

The demarcation of seasons in this part of the world is generally based upon the southwest monsoon. June–

September is considered as the monsoon period, October–January falls under the post-monsoon season, while February–May is considered to be the pre-monsoon season. The discrete monthly composite images for the four months of each season in a particular year were averaged by the model maker tool and a single image was produced for each season of each year. Colour coding was done on the respective images by classifying the datasets into 4–5 major groups; namely low, moderate, high and very high, to understand the spatial dynamics of these clusters over the season and the years studied.

Statistical analysis

Pearson correlation coefficient was calculated and accordingly, a correlation matrix was prepared amongst the five parameters studied, separately for ABS and BoB, with the aid of SPSS software package (version 16).

Limitations of the present study

It is noteworthy that *in situ* validation of the remotely sensed datasets of the study area, is out of the ambit of the present study, as two large areas have been considered. Moreover, MODIS data have a wide range of reported uncertainties and accuracies. Esaias *et al.*[15] reported an uncertainty of ± 1–2% for water-leaving spectral radiance and less than ± 0.2 K for SST brightness temperature of MODIS. An uncertainty of 0.2–0.4 K in

Table 1. Mean ± standard deviation along with range of biogeochemical parameters computed from the total monthly composite dataset from July 2002 to November 2014 in the Bay of Bengal (BoB) and Arabian Sea (ABS)

Parameters	Bay of Bengal	Arabian Sea
SST (°C)	28.93 ± 0.76 (22.77–35.78)	27.76 ± 1.12 (19.4–35.23)
PAR (mol m^{-2} d^{-1})	41.75 ± 3.75 (0.47–56.7)	45.76 ± 3.41 (20.31–57.83)
Chl-a (mg m^{-3})	0.187 ± 0.243 (0.010–55.830)	0.487 ± 0.984 (0.009–99.619)
POC (mg m^{-3})	57.82 ± 50.87 (16.6–12953.4)	117.83 ± 200.95 (16.2–12953.5)
PIC (mg m^{-3})	18.9 ± 74.3 (0.9–12275.9)	21.4 ± 32.1 (0.6–6202)

SST, Sea surface temperature; PAR, Photosynthetically active radiation; Chl a, Chlorophyll a; POC, Particulate organic carbon; PIC, Particulate inorganic carbon.

MODIS-derived SST has been reported by Kilpatrick *et al.*[25]. Based on the *in situ* validation of MODIS aqua satellite radiance, Moore *et al.*[26], corroborated a nominal uncertainty of ± 35% for global chlorophyll products, derived from NASA's ocean colour satellite program. Hu *et al.*[27] ascertained uncertainties and absolute accuracy of Chl-a derived from satellite ocean colour measurements. For blue bands and blue waters the uncertainty was within ± 5%, whereas for green bands it increased between 10% and 15% in case of oligotrophic water. Similarly, MODIS-derived PAR products are known to have an error of 2–3% (ref. 28). Additionally, it should also be mentioned that valid data exist only for cloud-free pixels and the monthly composite value stands for an average of cloud-free acquisitions for each ocean pixel. In pre-monsoon and post-monsoon season, cloud-free pixels in ABS and BoB ranged between 85% and 95%. However, during the monsoon season the availability of cloud-free pixels was sometimes as low as 10%.

Hence, keeping in mind the wide range of uncertainties for different parameters studied, the present study is only a semi-quantitative assessment. However, since the main objective of this study is comparative in nature along with spatio-temporal trend analysis, and since the uncertainties remains more or less same for all the used datasets for both the basins, we believe, that the main focus has not been hampered by the above-mentioned drawbacks.

Results and discussion

Overall comparison of 10-year composite mean dataset

Computation of overall mean of all the monthly composite data has revealed that SST in BoB is slightly higher than ABS. SST in BoB was found to be 28.93 ± 0.76°C, while in ABS it was 27.76 ± 1.12°C (Table 1). However, the magnitude of PAR recorded in ABS (45.76 ± 3.41 mol m^{-2} d^{-1}) was more compared to that in BoB (41.75 ± 3.75 mol m^{-2} d^{-1}). The mean Chl-a ~2.5 times more in ABS (0.487 ± 0.984 mg m^{-3}) than that observed in BoB (0.187 ± 0.243 mg m^{-3}). POC concentration in the surface waters of ABS (117.83 ± 200.95 mg m^{-3}) was

more than double compared to that in BoB (57.82 ± 50.87 mg m^{-3}). Unlike POC, PIC concentration in ABS (21.4 ± 32.1 mg m^{-3}) was marginally higher than that in the BoB (18.9 ± 74.3 mg m^{-3}).

Seasonal variability

Expectedly, the SST was highest during pre-monsoon season in both ABS and BoB, while in monsoon and post-monsoon it remains almost same. The seasonal composite mean data from 2002 to 2014, show the same trend during all the three seasons (Table 2). Analysing the datasets, it could be observed that for all the months the mean SST of ABS was invariably lower than that in BoB. The difference in SST between ABS and BoB was highest during monsoon season (~1.7°C), followed by the pre-monsoon season (~1.0°C), and the least during the post-monsoon season (~0.8°C). However, the standard deviation from the mean in case of ABS was found to be higher than BoB (Figure 2 *a*). This shows that SST varies over a wider range in ABS compared to BoB. Shenoi *et al.*[29], while characterizing the heat budget near the sea surface of ABS and BoB, observed that winds blowing over ABS during the summer monsoon are strong enough to facilitate the transfer of heat to deeper layers, due to overturning and turbulent mixing and hence leading to lower SST. On the contrary, the winds associated with summer monsoon in BoB are so weak that they lead to sluggish oceanic circulation, giving rise to a shallow surface mixed layer that is stable and responds quickly to changes in the atmosphere, eventually leading to a steadily high SST compared to ABS[29].

The seasonal composite data of PAR exhibited the same trend during all the three seasons, in both ABS and BoB (Figure 2 *b*). PAR was found higher in ABS compared to BoB during all the seasons. The difference was highest in the monsoon season (~6.3 mol m^{-2} d^{-1}) followed by pre-monsoon season (~3.5 mol m^{-2} d^{-1}) and the lowest in post-monsoon season (~2.3 mol m^{-2} d^{-1}) (Table 2). This might be attributed to the fact that during monsoon, the freshwater flow in BoB increases substantially and the turbidity of the water column increases, which prevents PAR to penetrate the sea surface. The differential spatial extent of cloud cover over the two basins
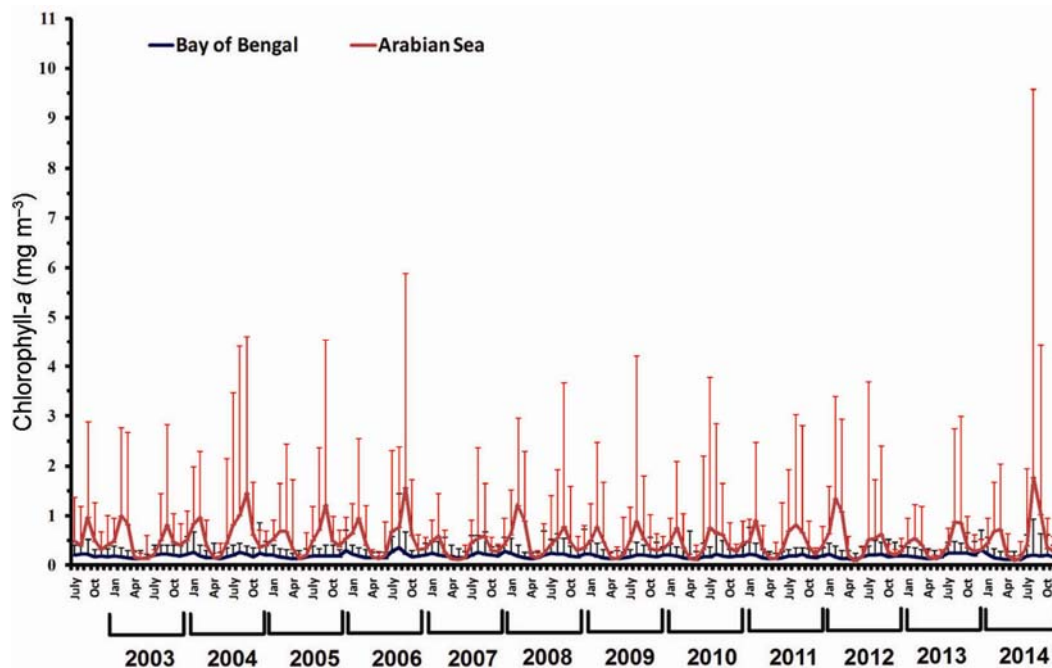
Table 2. Seasonal mean ± standard deviation along with the range of biogeochemical parameters computed from the average of monthly composite dataset of the respective seasons between July 2002 and November 2014 in BoB and ABS

Parameters	Pre-monsoon		Monsoon		Post-monsoon	
	BoB	ABS	BoB	ABS	BoB	ABS
SST (°C)	29.31 ± 0.89	28.32 ± 1.11	28.97 ± 0.68	27.22 ± 1.34	28.49 ± 0.70	27.73 ± 0.92
	(23.28–35.78)	(22.10–35.23)	(22.77–35.18)	(19.40–34.04)	(22.79–34.19)	(22.63–32.90)
PAR (mol m^{-2} d^{-1})	47.44 ± 3.32	50.94 ± 2.54	39.03 ± 5.05	45.39 ± 4.95	38.74 ± 2.84	41.10 ± 2.67
	(10.57–56.70)	(28.63–57.83)	(13.08–56.06)	(20.31–57.79)	(0.47–53.66)	(21.98–52.22)
Chl-a (mg m^{-3})	0.15 ± 0.19	0.43 ± 0.73	0.20 ± 0.27	0.61 ± 1.70	0.20 ± 0.27	0.41 ± 0.49
	(0.01–55.24)	(0.01–92.31)	(0.01–53.11)	(0.01–99.62)	(0.02–55.83)	(0.01–61.60)
POC (mg m^{-3})	50.64 ± 49.83	97.33 ± 121.99	59.9 ± 42.1	151.3 ± 366.3	62.74 ± 61.63	103.08 ± 107.54
	(16.6–12953.4)	(16.8–12953.4)	(17.8–12953.4)	(16.2–12953.5)	(19.4–12953.4)	(17.6–12953.4)
PIC (mg m^{-3})	15.40 ± 69.55	18.81 ± 36.07	22.16 ± 56.82	25.05 ± 23.63	18.79 ± 97.88	20.15 ± 37.40
	(0.9–12275.9)	(0.9–3959.9)	(0.9–8490.9)	(0.6–1775.0)	(0.9–11501.0)	(0.9–6202.0)

Figure 2. Monthly mean (*a*) sea-surface temperature (SST) and (*b*) photosynthetically active radiation (PAR) from July 2002 till November 2014 (error bars show the standard deviation from the mean).

could also be a decisive factor. Prasannakumar et al.[30] while exploring the reason behind reduced primary productivity in BoB, examined the status of PAR and concluded that the suspended sediment-laden riverine influx into BoB significantly curtailed the downward penetration of solar radiation. Moreover, they observed that the predominance of cloud cover also reduces the PAR, especially near the northern BoB[30].

The seasonal average showed that Chl-a concentration of BoB was more or less the same in the monsoon and post-monsoon season (0.20 ± 0.27 mg m^{-3}), while in the pre-monsoon season, it was quite low (0.15 ± 0.19 mg m^{-3}). The available data suggest that the Chl-a concentration in

ABS was substantially higher than BoB during all the seasons. The highest difference was found in the monsoon season (0.61 ± 1.70 mg m^{-3}), whereas in the pre-monsoon and post-monsoon season it was almost the same (~0.41 mg m^{-3}). Not only the mean, the standard deviation also varied over a wider range in ABS compared to BoB. This shows that extremely high Chl-a zones are quite abundant in ABS, and around September and February, a sudden increase in Chl-a concentration is observed in all the years over ABS (Figure 3). Previous studies found that several areas of ABS experience algal bloom during the northwest summer monsoon (i.e. August and September)[31,32] and the winter monsoon

Figure 3. Monthly mean chlorophyll-*a* (Chl-*a*) concentration from July 2002 till November 2014 (error bars show the standard deviation from the mean).
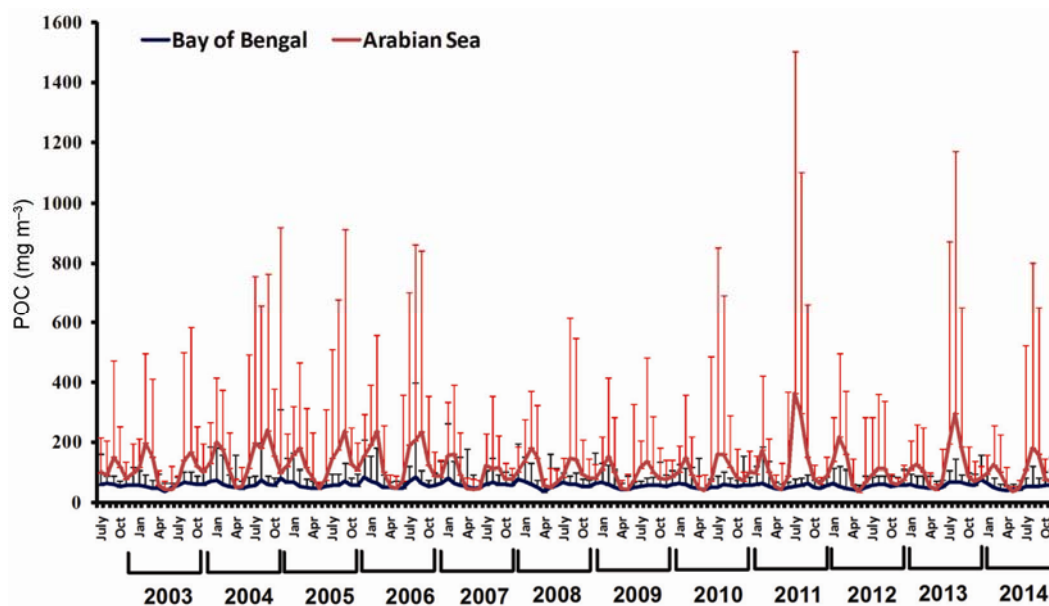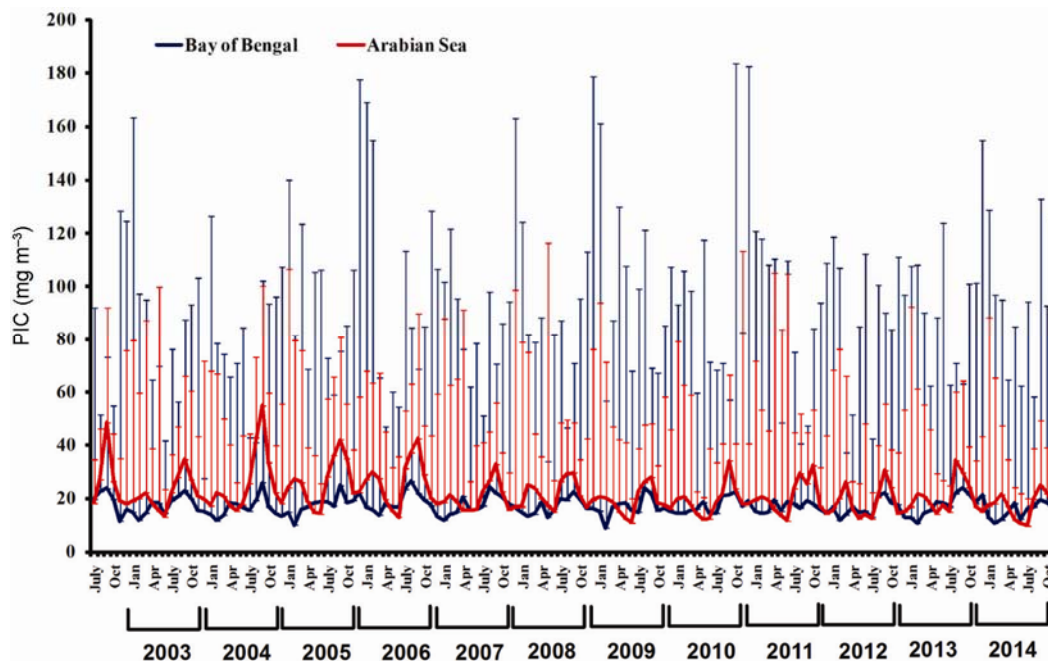

Figure 4. Monthly mean particulate organic carbon (POC) from July 2002 till November 2014 (error bars show the standard deviation from the mean).

(i.e. February and March)[33,34]. Hence our present finding is in conformity with the observed results of the past studies. The higher abundance of Chl-*a* concentration in ABS compared to BoB has also been confirmed by means of several *in situ* studies, as well as remotely sensed datasets[7,35,36].

Like Chl-*a*, POC also showed a sudden enhancement in concentration during September and February in ABS,

while no such trend was visible in case of BoB (Figure 4). Figure 4 is almost a prototype of the Chl-*a* map in case of both ABS and BoB, which shows that Chl-*a* and POC are spatially distributed in a similar way in both the basins. Figure 4 also shows that not only the mean but standard deviation is higher in ABS, which implies that POC has a wider range of data variability in ABS. In terms of magnitude, maximum difference between ABS

Figure 5. Monthly mean particulate inorganic carbon (PIC) from July 2002 till November 2014 (error bars show the standard deviation from the mean).
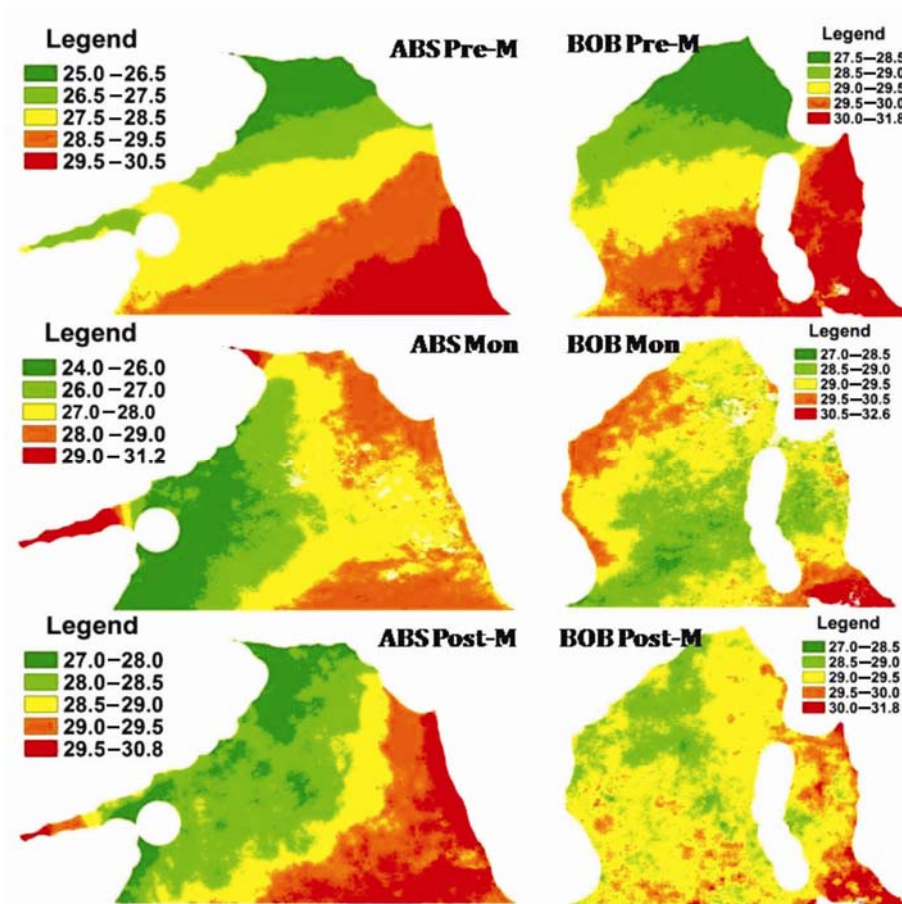
Figure 6. Maps showing the spatial distribution of SST (°C) in pre-monsoon, monsoon and post-monsoon season in ABS and BoB.
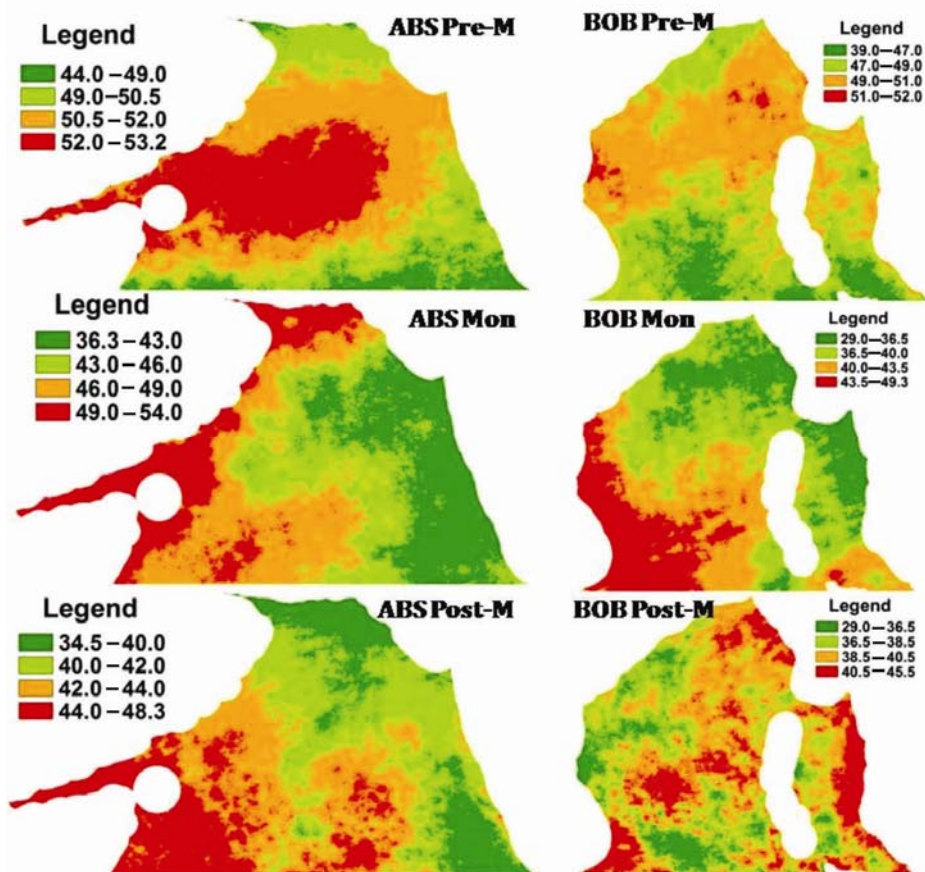
Figure 7. Maps showing the spatial distribution of PAR (mol m^{-2} d^{-1}) in pre-monsoon, monsoon and post-monsoon season in ABS and BoB.
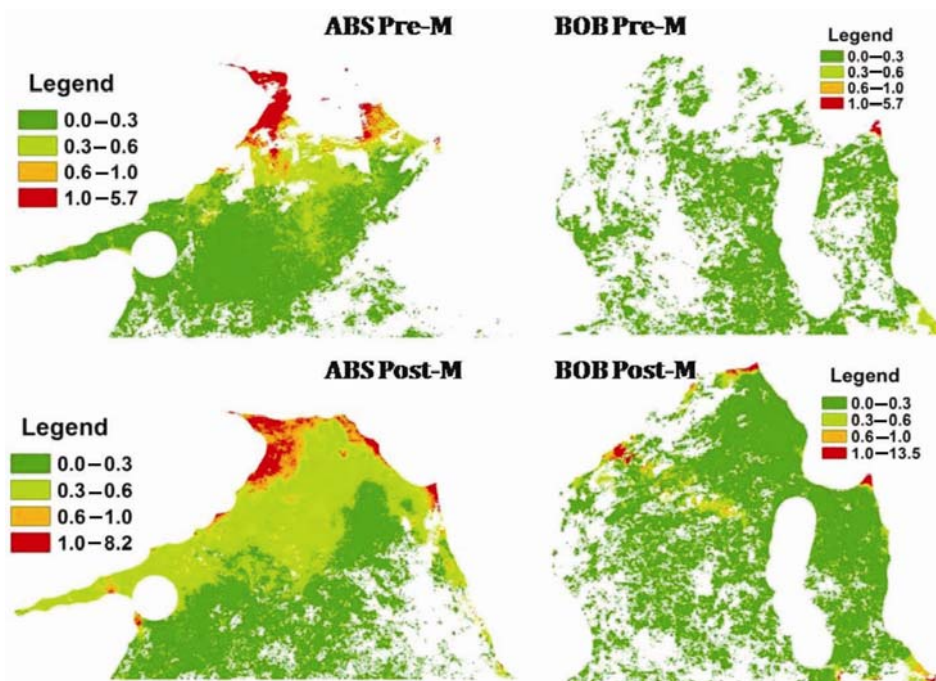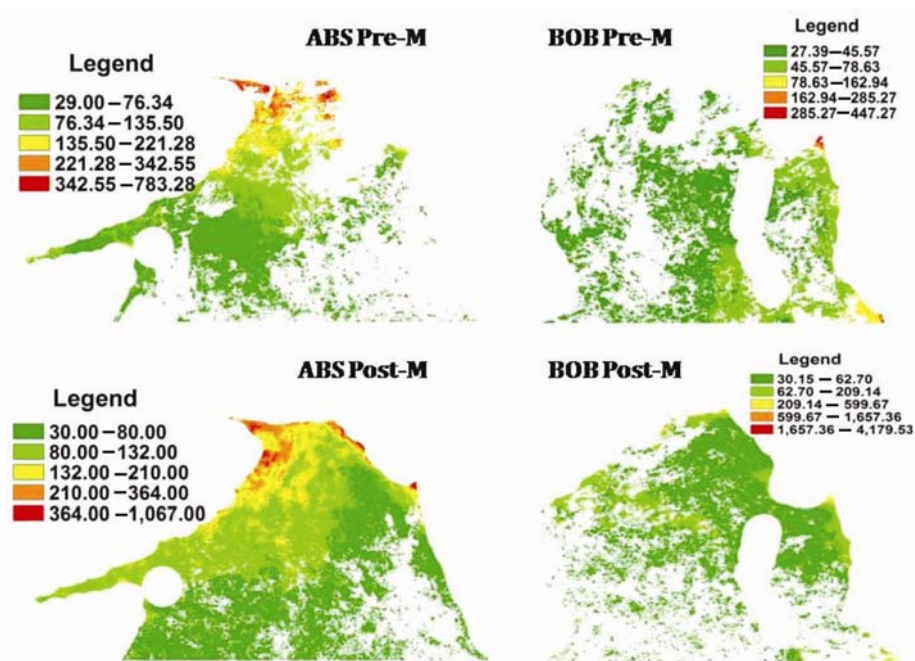

Figure 8. Maps showing the spatial distribution of Chl-*a* (mg m^{-3}) in pre-monsoon and post-monsoon season in ABS and BoB.

Figure 9. Maps showing the spatial distribution of POC (mg m^{-3}) in pre-monsoon and post-monsoon season in ABS and BoB.
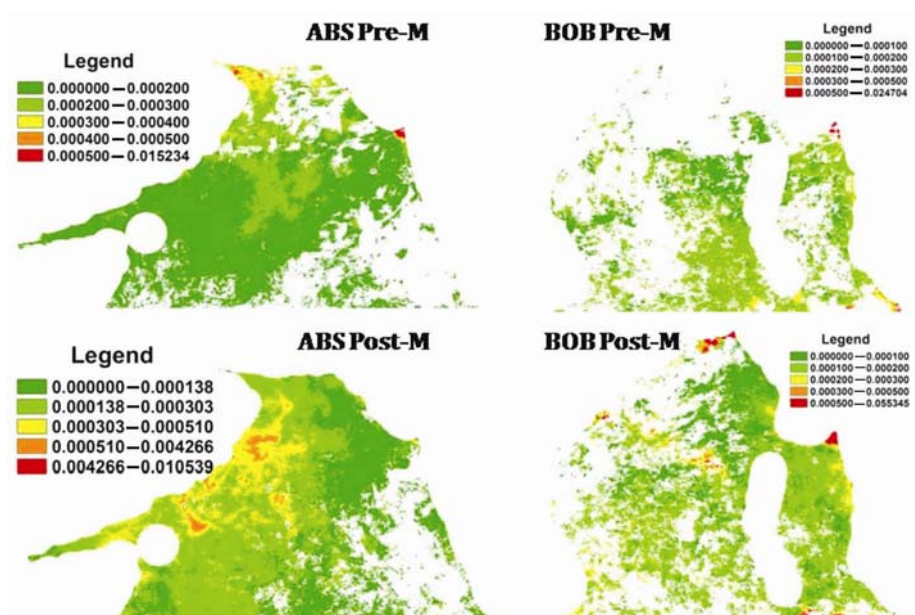
Figure 10. Maps showing the spatial distribution of PIC (mol m^{-3}) in pre-monsoon and post-monsoon season in ABS and BoB.

and BoB was observed during the monsoon, while it was quite low in case of pre- and post-monsoon season. Very few studies based on *in situ* measurement of POC have been reported from these regions. However, the observations of Fernandes *et al.*[37], regarding magnitude of POC in various sites of BoB were found to be parity with our remotely sensed data. Similarly, earlier studies by Gundersen *et al.*[38] and Gardner *et al.*[39] carried out on ABS,

showed comparable results with those of our observations.

In all the three seasons, the difference in PIC concentration was more or less constant; however, it was least in the post-monsoon season (~1.36 mg m^{-3}). Figure 5 depicts that unlike the other parameters discussed so far, PIC is the only parameter which shows greater variability in BoB compared to ABS, which is denoted by the longer
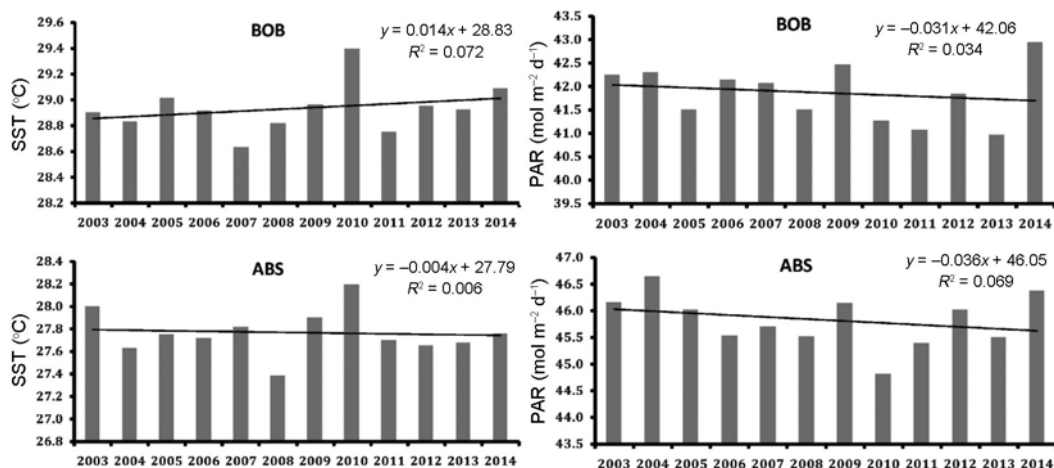
Figure 11. The temporal trend of SST and PAR between the years 2003 and 2014 in ABS and BoB.
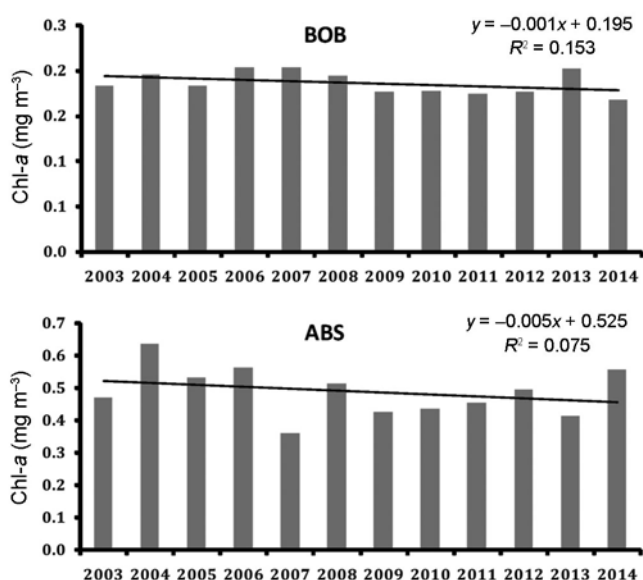

Figure 12. The temporal trend of Chl-*a* between the years 2003 and 2014 in ABS and BoB.

error bars depicting the standard deviation from the mean.

Spatial variability

The spatial distribution maps of SST (Figure 6) portray that in ABS comparatively higher temperatures were always observed towards the Indian coast and near the Arabian coast, whereas in Iranian and Pakistan coast, comparatively lower temperature waters were found to prevail. Izumo *et al.*[40], observed that coastal upwelling along the Somalia and Oman coasts starts during late spring, peaks during the summer monsoon, and eventually cools the SST in the western ABS. In the pre-monsoon season the demarcation of cooler to warmer water regions

in ABS was prominent from the Iranian coast to south-western Indian coast. In BoB, such demarcation was also observed in the pre-monsoon season with comparatively cooler waters in the northern BoB and warmer waters towards the south, especially near Andaman & Nicobar Islands. In the monsoon and post-monsoon, there was no such fixed trend in BoB.

The spatial distribution maps of PAR over ABS clearly depict that, higher PAR was found to exist near the Somalian coast and the coast of Yemen and Oman (Figure 7). In the pre-monsoon season, a substantial portion of the central Arabian Sea received a PAR of 52–53 mol m^{-2} d^{-1}. In the monsoon season, the high PAR zones were mainly found near the coastlines, while in the post-monsoon season, this zone moved more towards the equator. In case of BoB, in the pre-monsoon season, sub-stantially higher values of PAR were observed in the cen-tral and northern portion, except near the confluence of River Ganga. During monsoon, this zone moved towards the south of the eastern coast and near Sri Lanka, while in the post-monsoon season, PAR varied over a wide range, and the high and low PAR areas were scattered all through BoB.

Due to extensive cloud cover, composite maps of Chl-*a* could not be prepared for the monsoon season. In the pre-monsoon and post-monsoon season, higher Chl-*a* values were observed near the Gulf of Oman and up to the cen-tral Arabian Sea substantially moderate values were observed to exist (Figure 8). While in BoB, the whole basin showed lower values consistently throughout the entire region. Dey and Singh[35] also observed such higher concentrations of Chl-*a* in the coastal waters compared to open ocean. However, in the post-monsoon season, a stretch of high Chl-*a* zone transversing to the east coast of India, was observed to exist. In this regard, it is worth mentioning that BoB experiences several cyclones and its passé co-exists with this tract of enhanced Chl-*a* concen-tration. Lotliker *et al.*[41] observed substantially enhanced
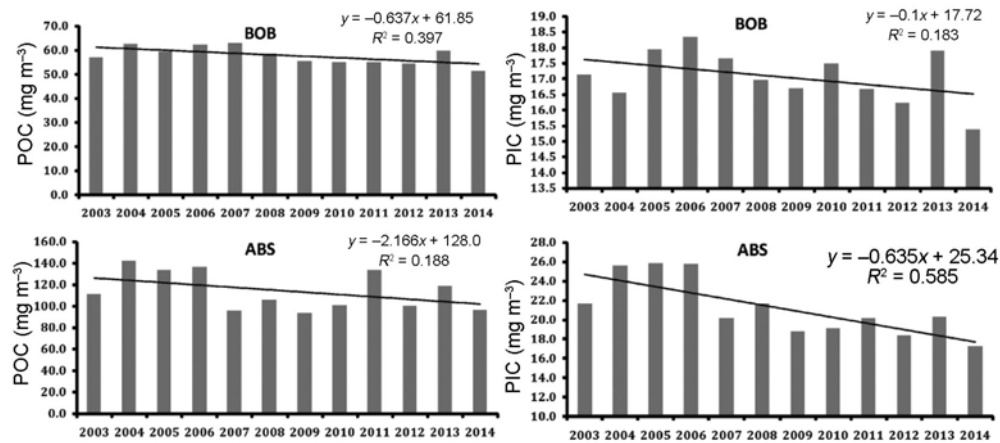
Figure 13. The temporal trend of POC and PIC between the years 2003 and 2014 in ABS and BoB.

Table 3. Pearson correlation coefficient matrix between the five bio-geochemical parameters studied in ABS

Parameters		SST	Chl-*a*	POC	PAR	PIC
SST	Pearson correlation	1				
	Significant (two-tailed)					
Chl-*a*	Pearson correlation	–0.663**	1			
	Significant (two-tailed)	0.000				
POC	Pearson correlation	–0.693**	0.820**	1		
	Significant (two-tailed)	0.000	0.000			
PAR	Pearson correlation	0.391**	–0.111	–0.177*	1	
	Significant (two-tailed)	0.000	0.178	0.031		
PIC	Pearson correlation	–0.414**	0.649**	0.619**	–0.004	1
	Significant (two-tailed)	0.000	0.000	0.000	0.958	

**Correlation is significant at the 0.01 level (two-tailed; $n = 149$). *Correlation is significant at the 0.05 level (two-tailed).

Chl-*a* concentration in this tract while studying the after effects of Cyclone *Phailin*. Figure 9 portraying the spatial variability of POC, is almost a prototype of Chl-*a* map in case of both ABS and BoB, which shows that Chl-*a* and POC were spatially distributed in a similar way in both the basins. Figure 10 shows that the orange to red regions denoting higher values of PIC, are found near the Gulf of Oman in the pre-monsoon season, and in the northwestern and central ABS in the post-monsoon season. In BoB, these regions of high PIC were scarcely observed in the pre-monsoon season, except near the coastline of Myanmar and the south of Andaman Sea. However, in post-monsoon season, in addition to these spots, high PIC regions were observed near the confluence of River Ganga and along the same transverse tract where high Chl-*a* concentration was observed in the same season. Figure 10 shows that consistently in the post-monsoon season, the PIC concentration of BoB and ABS has remained fairly the same.

Decadal trend

The annual mean values were plotted in the respective years and the trend of the variation was assessed in case

of all the parameters separately for BoB and ABS. Analysing the temporal variability of the annual mean data, it was observed that SST and PAR did not show any significant trend in the last decade (Figure 11). There was no noteworthy trend in case of Chl-*a* also (Figure 12). However, the only reportable significant decadal trend was observed in case of PIC in ABS (Figure 13). PIC has shown a decreasing trend in these 12 years which might be an indicator of the onset of ocean acidification as recently observed by Freeman and Lovenduski[42] while working in the Southern Ocean. However, it is not suitable to draw any firm conclusion just from the dataset of 12 years.

Correlation between the selected parameters

Combining the total decadal data, Pearson correlation coefficient was calculated among the parameters studied in both ABS (Table 3) and BoB (Table 4). In case of BoB, all the possible correlations were found to be statistically significant (99% significance level), while in case of ABS, except for the relation between PAR and Chl-*a*

Table 4. Pearson correlation coefficient matrix between the five bio-geochemical parameters studied in BoB

Parameters		SST	Chl-*a*	POC	PAR	PIC
SST	Pearson correlation	1				
	Significant (two-tailed)					
Chl-*a*	Pearson correlation	–0.595**	1			
	Significant (two-tailed)	0.000				
POC	Pearson correlation	–0.681**	0.928**	1		
	Significant (two-tailed)	0.000	0.000			
PAR	Pearson correlation	0.348**	–0.544**	–0.462**	1	
	Significant (two-tailed)	0.000	0.000	0.000		
PIC	Pearson correlation	0.277**	0.398**	0.239**	–0.285**	1
	Significant (two-tailed)	0.001	0.000	0.003	0.000	

**Correlation is significant at the 0.01 level (two-tailed; $N = 149$).

along with PAR and PIC, all the others were statistically significant. SST and Chl-*a* were negatively correlated in both ABS and BoB, with higher degree in ABS. A negative correlation between PAR and Chl-*a* was also observed in BoB. This shows that Chl-*a* abundance depends on the optimum temperature; too much increase in temperature actually decreases the Chl-*a* content in the surface. Since sunrays mainly act as the cause of ambient water temperature, which is also the source of PAR, the same type of relation was found between PAR and Chl-*a* too. Apart from these, a strong correlation was obtained between Chl-*a* and POC, as Chl-*a* itself contributed to a substantial portion of POC.

Conclusion

The present study was carried out to monitor the status of two important regions of the Indian Ocean namely, ABS and BoB, in the last decade from the perspective of five selected bio-geochemical parameters, using a remote sensing approach. Combining the principal outcomes obtained from this study, it can be inferred that ABS on the whole is marginally cooler than BoB, and this difference is maintained in all the three seasons. Spatially, SST was found to vary with lower temperatures away from the equator. This trend was found throughout in ABS; however, in BoB it was not so clearly demarcated. Unlike SST, ABS had a higher PAR compared to BoB. The range of PAR varied over seasons and the spatial distribution could be mainly justified by cloud cover and turbidity of the water column. Chl-*a* concentration in the surface waters of ABS was found almost two and a half times more than that observed in BoB. The variability of Chl-*a* was also substantially high in ABS compared to BoB. The north ABS, especially near the Gulf of Oman, recorded very high Chl-*a* concentration and it was found to steadily decrease towards the south. BoB mostly had a fairly low Chl-*a* concentration, except near the Andhra Pradesh coastline, few patches near the Ganges confluence and near Myanmar. Along with Chl-*a*, both POC

and PIC were found higher in ABS compared to BoB. POC was substantially high; however, PIC was marginally high. The spatial dynamics of POC was almost a prototype of Chl-*a* variability. All the five parameters correlated well with each other in both the basins. POC exhibited strong positive correlation with Chl-*a*, while SST and PAR showed a negative correlation with Chl-*a*. The study of temporal trend of these parameters exhibits a decreasing trend of PIC in ABS over the last decade, which might be an indication of ocean acidification in its rudimentary stage.

1. Tilstone, G. H., Angel-Benavides, I. M., Pradhan, Y., Shutler, J. D., Groom, S. and Sathyendranath, S., An assessment of chlorophyll-*a* algorithms available for *SeaWiFs* in coastal and open areas of the Bay of Bengal and Arabian Sea. *Remote Sensing Environ.*, 2011, **115**, 2277–2291.
2. Holm-Hansen, O. *et al.*, Temporal and spatial distribution of chlorophyll-*a* in surface waters of the Scotia Sea as determined by both shipboard measurements and satellite data. Deep-Sea Res. II, 2004, **51**, 1323–1331.
3. Moses, W. J., Gitelson, A. A., Berdnikov, S. and Povazhnyy, V., Estimation of chlorophyll-*a* concentration in case II waters using MODIS and MERIS data – successes and challenges. *Environ. Res. Lett.*, 2009, **4**, 1–8.
4. Jaswal, A. K., Singh, V. and Bhambak, S. R., Relationship between sea surface temperature and surface air temperature over Arabian Sea, Bay of Bengal and Indian Ocean. *J. Indian Geophys. Union*, 2012, **16**, 41–53.
5. Grossant, H. P. and Ploug, H., Microbial degradation of organic carbon and nitrogen on diatom aggregates. *Limnol. Oceanogr.*, 2001, **46**, 267–277.
6. Eppley, R. W. and Peterson, B. J. Particulate organic matter flux and planktonic new production in the deep ocean. *Nature*, 1979, **282**, 677–680.
7. Gauns, M., Madhupratap, M., Ramaiah, N., Jyothibabu, R., Fernandes, V., Paul, J. T. and Prasanna Kumar, S., Comparative accounts of biological productivity characteristics and estimates of carbon fluxes in the Arabian Sea and the Bay of Bengal. *Deep-Sea Res. II*, 2005, **52**, 2003–2017.
8. UNESCO, River inputs to the ocean systems: status and recommendations for research. In UNESCO Technical Papers in Marine Science, No. 55, Final Report of the SCOR Working Group 46, Paris, 1988, p. 25.
9. Subramanian, V., Sediment load of Indian rivers. *Curr. Sci.*, 1993, **64**, 928–930.

10. Prasanna Kumar, S. *et al.*, Why is the Bay of Bengal less productive during summer monsoon compared to the Arabian Sea? *Geophys. Res. Lett.*, 2002, **29**, 2235; doi: 10.1029/2002GL016013.

11. Gill, A. E., *Atmosphere Ocean Dynamics*, Academic Press, New York, 1982.

12. Paul, J. T., Ramaiah, N., Gauns, M. and Fernandes, V., Preponderance of a few diatom species among the highly diverse microphytoplankton assemblages in the Bay of Bengal. *Mar. Biol.*, 2007, **152**, 63–75.

13. Dietrich, G., The unique situation in the environment of the Indian Ocean. In *The Biology of the Indian Ocean* (ed. Zeitzschel, B.), Springer, Berlin, 1973, pp. 1–6.

14. Madhupratap, M. *et al.*, Biogeochemistry of the Bay of Bengal: physical, chemical and primary productivity characteristics of the central and western Bay of Bengal during summer monsoon. *Deep-Sea Res. II*, 2003, **50**, 881–896.

15. Esaias, W. E. *et al.*, An overview of MODIS capabilities for ocean science observations. *IEEE Trans. Geosci. Remote Sensing*, 1998, **36**, 1250–1265.

16. Salomonson, V., Guenther, B. and Masuoka, E., A summary of the status of the EOS Terra Mission Moderate Resolution Imaging Spectroradiometer (MODIS) and attendant data product development after one year of on-orbit performance. In Proceedings of the International Geoscience and Remote Sensing Symposium, Sydney, Australia, 2001.

17. Savtchenko, A., Ouzounov, D., Ahmad, S., Acker, J., Leptoukh, G., Koziana, J. and Nickless, D., Terra and Aqua MODIS products available from NASA GES DAAC. *Adv. Space Res.*, 2004, **34**, 710–714.

18. http://www.britannica.com/EBchecked/topic/31653/Arabian-Sea (accessed on 4 February 2015).

19. http://www.britannica.com/EBchecked/topic/60740/Bay-of-Bengal (accessed on 4 February 2015).

20. Laruelle, G. G., Dürr, H. H., Slomp, C. P. and Borges, A. V., Evaluation of sinks and sources of CO_2 in the global coastal ocean using a spatially-explicit typology of estuaries and continental shelves. *Geophys. Res. Lett.*, 2010, **37**, L15607; doi: 10.1029/2010GL043691.

21. Morel, A. and Prieur, L., Analysis of variations in ocean color. *Limnol. Oceanogr.*, 1977, **22**, 709–722.

22. Dall'Olmo, G., Gitelson, A. A., Rundquist, D. C., Leavitt, B., Barrow, T., and Holz, J. C., Assessing the potential of SeaWiFS and MODIS for estimating chlorophyll concentration in turbid productive waters using red and near-infrared bands. *Remote Sensing Environ.*, 2005, **96**, 176–187.

23. Darecki, M. and Stramski, D., An evaluation of MODIS and Sea-WiFS bio-optical algorithms in the Baltic Sea. *Remote Sensing Environ.*, 2004, **89**, 326–350.

24. O'Reilly, J. E. and 24 co-authors, SeaWiFS Postlaunch Calibration and Validation Analyses, Part 3. In NASA Tech. Memo. 2000–206892 (eds Hooker, S. B. and Firestone, E. B.), NASA Goddard Space Flight Center, vol. 11, 2000, p. 49.

25. Kilpatrick, K. A. *et al.*, A decade of sea surface temperature from MODIS. *Remote Sensing Environ.*, 2015, **165**, 27–41.

26. Moore, T. S., Campbell, J. W. and Dowell, M. D., A class-based approach to characterizing and mapping the uncertainty of the MODIS ocean chlorophyll product. *Remote Sensing Environ.*, 2009, **113**, 2424–2430.

27. Hu, C., Feng, L. and Lee, Z. Uncertainties of SeaWiFS and MODIS remote sensing reflectance: Implications from clear water measurements. *Remote Sensing Environ.*, 2013, **133**, 168–182.

28. Van Laake, P. E. and Sanchez-Azofeifa, G. A., Simplified atmospheric radiative transfer modelling for estimating incident PAR using MODIS atmosphere products. *Remote Sensing Environ.*, 2004, **91**, 98–113.

29. Shenoi, S. S. C., Shankar, D. and Shetye, S. R., Differences in heat budgets of the near-surface Arabian Sea and Bay of Bengal: implications for the summer monsoon. *J. Geophys. Res.: Oceans* 2002, **107**, 5–1.

30. Prasannakumar, S. *et al.*, Is the biological productivity in the Bay of Bengal light limited? *Curr. Sci.*, 2010, **98**, 1331–1339.

31. Brock, J. and McClain, C., Interannual variability in phytoplankton blooms observed in the northwestern Arabian Sea during the southwest monsoon. *J. Geophys. Res.*, 1992, **97**, 733–750.

32. Madhupratap, M., Sawant, S. and Gauns, M., A first report on a bloom of the marine prymnesiophycean, *Phaeocystis globosa* from the Arabian Sea. *Oceanol. Acta*, 2000, **23**, 83–90.

33. Sarangi, R. K., Chauhan, P. and Nayak, S. R., Inter-annual variability of phytoplankton blooms in the northern Arabian Sea during winter monsoon period (February–March) using IRS-P4 OCM data. *Indian J. Mar. Sci.*, 2005, **34**, 163–173.

34. Sarangi, R. K., Observation of algal bloom in the northwest Arabian Sea using multisensor remote sensing satellite data. *Mar. Geod.*, 2012, **35**, 158–174.

35. Dey, S. and Singh, R. P., Comparison of chlorophyll distributions in the northeastern Arabian Sea and southern Bay of Bengal using IRS-P4 Ocean Color Monitor data. *Remote Sensing Environ.*, 2003, **85**, 424–428.

36. Pattabiraman, V., Munavar, M. and Suresh, K., Comparative study on chlorophyll distributions in the coastal regions of northeastern Arabian Sea and southern Bay of Bengal based on Indian seasons and rainfall distributions. In Asia Pacific Conference on Environmental Science and Technology, Advances in Biomedical Engineering, 2012, vol. 6, pp. 453–458.

37. Fernandes, L., Bhosle, N. B., Matondkar, S. P. and Bhushan, R., Seasonal and spatial distribution of particulate organic matter in the Bay of Bengal. *J. Mar. Syst.*, 2009, **77**, 137–147.

38. Gundersen, J. S., Gardner, W. D., Richardson, M. J. and Walsh, I. D., Effects of monsoons on the seasonal and spatial distributions of POC and chlorophyll in the Arabian Sea. *Deep-Sea Res. II*, 1998, **45**, 2103–2132.

39. Gardner, W. D., Mishonov, A. V. and Richardson, M. J., Global POC concentrations from *in situ* and satellite data. *Deep Sea Res. II*, 2006, **53**, 718–740.

40. Izumo, T., Montégut, C. B., Luo, J. J., Behera, S. K., Masson, S. and Yamagata, T. The role of the western Arabian Sea upwelling in Indian monsoon rainfall variability. *J. Climate*, 2008, **21**, 5603–5623.

41. Lotliker, A. A., Kumar, T. S., Reddem, V. S. and Nayak, S., Cyclone Phailin enhanced the productivity following its passage: evidence from satellite data. *Curr. Sci.*, 2014, **106**, 360–361.

42. Freeman, N. M. and Lovenduski, N. S., Decreased calcification in the Southern Ocean over the satellite record. *Geophys. Res. Lett.*, 2015, **42**, 1834–1840.